

The evolution of sex-specific immune defences

Olivier Restif & William Amos

Electronic Supplementary Material

Appendix S1. Analysis of the population dynamic model

1. When a single host genotype is present in the population, the dynamics of the system are described by the following system of differential equations:

$$\begin{cases} \frac{dS_f}{dt} = \frac{1}{2}b(1-qN)S_f - d_f S_f - \beta_f S_f(I_f + I_m) + \gamma_f I_f \\ \frac{dS_m}{dt} = \frac{1}{2}b(1-qN)S_f - d_m S_m - \beta_m S_m(I_f + I_m) + \gamma_m I_m \\ \frac{dI_f}{dt} = \beta_f S_f(I_f + I_m) - (\gamma_f + \alpha_f + d_f)I_f \\ \frac{dI_m}{dt} = \beta_m S_m(I_f + I_m) - (\gamma_m + \alpha_m + d_m)I_m \end{cases} \quad (S1.1)$$

2. In the absence of pathogen and with a single host genotype, the stable equilibrium densities of females and males are: $S_f^* = \frac{d_m}{d_f + d_m} \frac{b - 2d_f}{bq}$; $S_m^* = \frac{d_f}{d_f + d_m} \frac{b - 2d_f}{bq}$.

So the carrying capacity is given by $S_f^* + S_m^* = \frac{b - 2d_f}{bq}$.

3. The basic reproductive ratio of the pathogen with a single host genotype is given by:

$$R_0 = \frac{\beta_f S_f^* + \beta_m S_m^*}{S_f^* + S_m^*} \left[\frac{S_f^*}{\gamma_f + \alpha_f + d_f} + \frac{S_m^*}{\gamma_m + \alpha_m + d_m} \right] \quad (S1.2)$$

Using the default numerical values listed in Table 1, we get $S_f^* = S_m^* = 25$ and $R_0 = 10/3 \approx 3.33$.

4. The basic reproductive ratio of the pathogen in the presence of multiple host genotypes (indexed by superscript i) is given by:

$$R_0 = \frac{\sum_i (\beta_f S_f^{i*} + \beta_m S_m^{i*})}{\sum_i (S_f^{i*} + S_m^{i*})} \sum_i \left[\frac{S_f^{i*}}{\gamma_f^i + \alpha_f^i + d_f^i} + \frac{S_m^{i*}}{\gamma_m^i + \alpha_m^i + d_m^i} \right] \quad (S1.3)$$

where S_f^{i*} and S_m^{i*} are the equilibrium densities of susceptible females and males with genotype i in the absence of infection.

Appendix S2. Evolutionary analysis at a single locus.

We carry out our analyses in two steps: first, we considered the evolution at each locus separately, and then their coevolution. In this appendix we use a number of standard techniques from adaptive dynamics theory; for the definition of terms, description of basic methods and an extensive list of references on the topic, please visit the Adaptive Dynamics Network website: <http://www.iiasa.ac.at/Research/ADN/AdaptiveDynamics.html>

1. Invasion analysis at a single locus.

We begin by fixing the value of the male traits at their default values (Table 1), i.e. assuming that a single allele is fixed at the ‘male’ locus. We focus on the evolution of the female proxy trait x_f using invasion analysis, which is the standard method in adaptive dynamics. When a resident allele A is fixed at the ‘female’ locus (remembering that both sexes carry this locus), we can estimate numerically the stable equilibrium point of system (S1.1). We can then assess the ability of any mutant allele A' to spread in the population by calculating the eigenvalues of the complete system (2) with 3 genotypes: AA with trait value x_A , $A'A'$ with trait value $x_{A'}$, and heterozygotes AA' with trait value $(x_A + x_{A'})/2$. If the real part of the dominant eigenvalue is positive, the mutant allele can spread, if it's negative the mutant allele vanishes.

We can explore the full range of trait values (from 0 to 1) for both resident and mutant alleles and produce a pairwise invasion plot, which provides a graphical indication of the existence and nature of evolutionarily singular points. In addition we can use a numerical algorithm to estimate the value of evolutionarily stable strategies (ESS) when one exists: the principle is, for any given resident allele A , to determine the mutant allele A^* with the highest dominant eigenvalue (or real part thereof); the algorithm searches for a resident A such that $A^* = A$. Indeed, such an allele cannot be invaded by any mutant, which is the definition of an ESS.

2. Pairwise Invasion Plots at a single locus.

Here we illustrate the evolutionary properties of different trade-off functions, first for females traits, then for male traits. For each of the three pairs of traits considered (see main text, section 2.a), we explored the behaviour of a few mathematical function linking these traits to the value of the proxy trait x_f or x_m . Only a few representative plots are presented below. Default numerical values for non-evolving parameters are in Table 1 in the main text. In the following plots, x_{res} designates the phenotype of the resident allele and x_{mut} that of the mutant allele; blue shades represent regions where the real part of the dominant eigenvalue is negative (no invasion) and brown shades (marked with a +) represent regions where the real part of the dominant eigenvalue is positive (invasion).

We encounter four types of singularities:

- continuously stable strategies, i.e. both evolutionarily and convergence stable;
- repeller, i.e. both evolutionarily and convergence unstable;
- ‘Garden of Eden’, i.e. evolutionarily stable but convergence unstable;
- branching point, i.e. evolutionarily unstable but convergence stable.

The last type has received a lot of attention in the adaptive dynamic literature because of its potential to explain the evolution of polymorphism or even sympatric speciation. However, with our model we only encountered branching points under very restrictive conditions.

Previous models for the evolution of asexual host indicated that intermediate investment in defences cannot be evolutionarily stable unless the cost of defences is an accelerating function of the investment in defences (Boots & Haraguchi 1999; Restif & Koella 2004). In contrast, we found that linear trade-off functions between recovery rate γ and mortality d (model i) or between relative fecundity during infection ϕ and mortality d (model ii) raised intermediate ESS. However, using linear functions in our third model (resistance-tolerance trade-off) raised an evolutionary repeller.

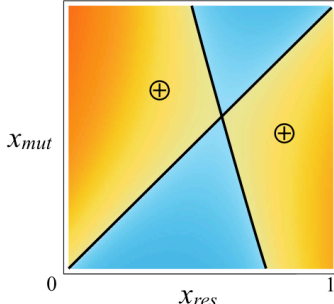
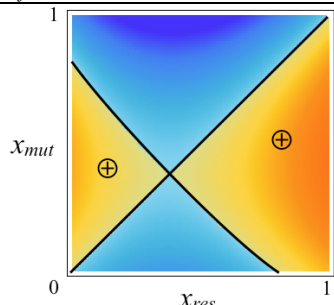
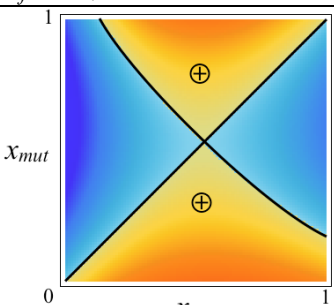
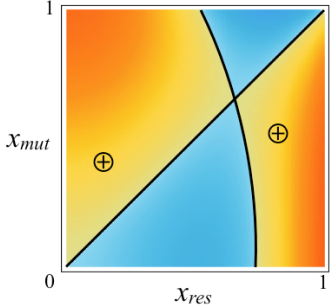
2.1. Female traits.

(i) Recovery rate vs. survival

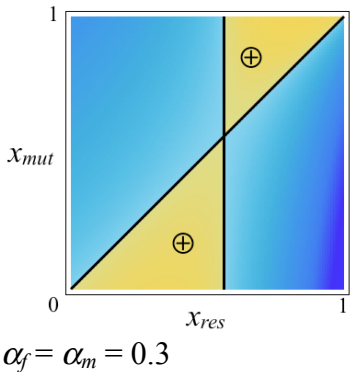
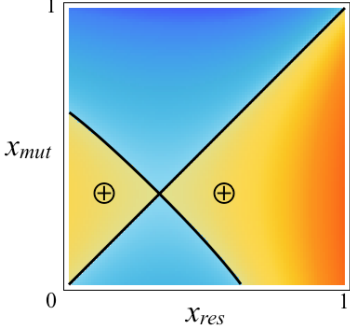
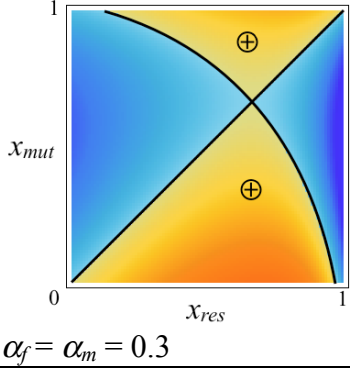
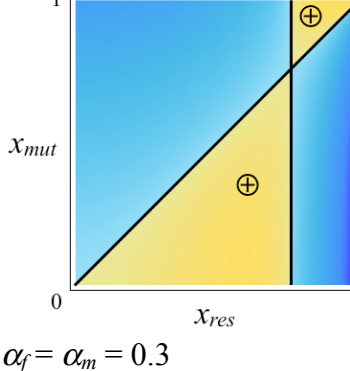
Trade-off functions	Exemplary invasion plot	Nature of the singularity ^a
Linear functions $\begin{cases} \gamma_f = \gamma_0(1 - x_f) \\ d_f = d_0(1 - x_f / 2) \end{cases}$		Evolutionarily stable and convergence-stable
Quadratic recovery rate $\begin{cases} \gamma_f = \gamma_0(1 - x_f^2) \\ d_f = d_0(1 - x_f / 2) \end{cases}$		Evolutionarily stable and convergence-stable
Quadratic death rate $\begin{cases} \gamma_f = \gamma_0(1 - x_f) \\ d_f = d_0(1 - x_f^2 / 2) \end{cases}$		Evolutionarily unstable and convergence-unstable.
	 $\alpha_f = \alpha_m = 0.37$	For a narrow range of parameter values, there are two singular points, both evolutionarily unstable: - x_1 is convergence-unstable (repellor), - x_2 is convergence-stable (branching point). Other parameter values (e.g. higher virulence) result in the two singular points to vanish.
Quadratic functions $\begin{cases} \gamma_f = \gamma_0(1 - x_f^2) \\ d_f = d_0(1 - x_f^2 / 2) \end{cases}$		

^a For definitions of the singularities, see for example Geritz et al. (1997).

(ii) Relative fecundity during infection vs. survival

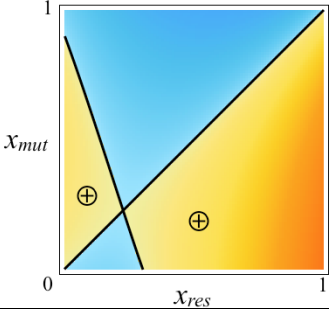
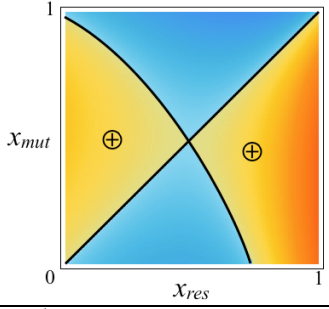
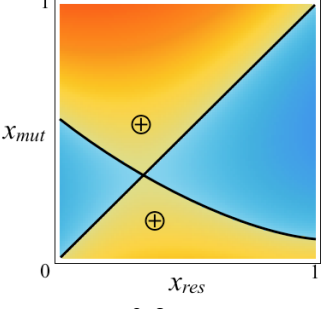
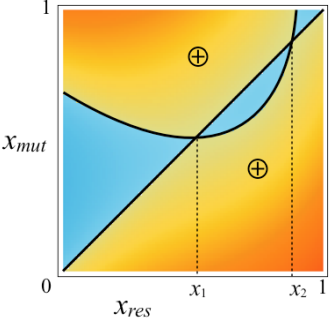
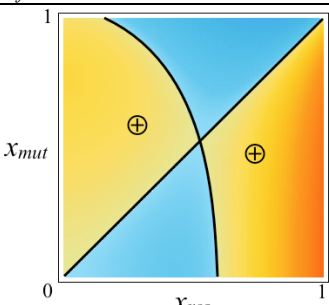
Trade-off functions	Exemplary invasion plot	Nature of the singularity
<p>Linear functions</p> $\begin{cases} \varphi_f = 1 - x_f \\ d_f = d_0 (1 - x_f / 2) \end{cases}$	 <p>$\alpha_f = \alpha_m = 0.54$</p>	<p>Evolutionarily stable and convergence-stable; only found over a narrow range of parameter values.</p>
<p>Quadratic fecundity</p> $\begin{cases} \varphi_f = 1 - x_f^2 \\ d_f = d_0 (1 - x_f / 2) \end{cases}$	 <p>$\alpha_f = \alpha_m = 0.4$</p>	<p>Evolutionarily stable and convergence-stable.</p>
<p>Quadratic death rate</p> $\begin{cases} \varphi_f = 1 - x_f \\ d_f = d_0 (1 - x_f^2 / 2) \end{cases}$		<p>Evolutionarily unstable and convergence-unstable (repellor).</p>
<p>Quadratic functions</p> $\begin{cases} \varphi_f = 1 - x_f^2 \\ d_f = d_0 (1 - x_f^2 / 2) \end{cases}$	 <p>$\alpha_f = \alpha_m = 0.53$</p>	<p>Evolutionarily stable and convergence-stable; only found over a narrow range of parameter values.</p>

(iii) Recovery vs. relative fecundity during infection

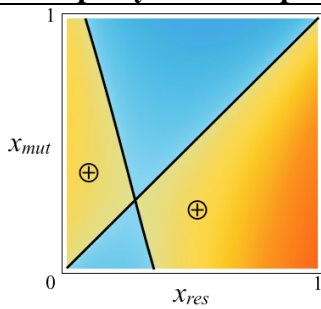
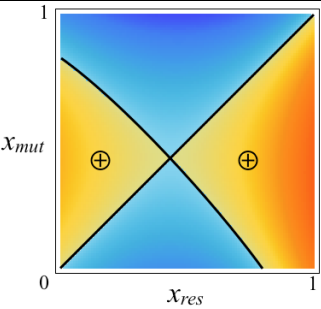
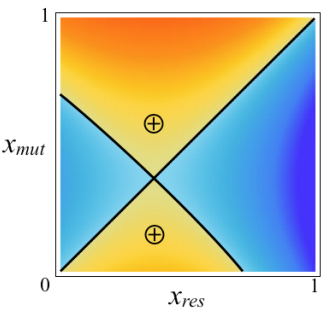
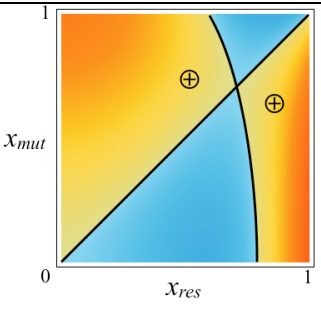
Trade-off functions	Exemplary invasion plot	Nature of the singularity
<p>Linear functions</p> $\begin{cases} \varphi_f = x_f \\ \gamma_f = \gamma_0(1 - x_f) \end{cases}$	 <p>$\alpha_f = \alpha_m = 0.3$</p>	<p>Evolutionarily neutral and convergence unstable ('Garden of Eden' singularity)</p>
<p>Quadratic recovery</p> $\begin{cases} \varphi_f = x_f \\ \gamma_f = \gamma_0(1 - x_f^2) \end{cases}$		<p>Evolutionarily stable and convergence-stable.</p>
<p>Quadratic fecundity</p> $\begin{cases} \varphi_f = x_f^2 \\ \gamma_f = \gamma_0(1 - x_f) \end{cases}$	 <p>$\alpha_f = \alpha_m = 0.3$</p>	<p>Evolutionarily unstable and convergence-unstable.</p>
<p>Quadratic functions</p> $\begin{cases} \varphi_f = x_f^2 \\ \gamma_f = \gamma_0(1 - x_f^2) \end{cases}$	 <p>$\alpha_f = \alpha_m = 0.3$</p>	<p>Evolutionarily neutral and convergence unstable.</p>

2.2. Male traits.

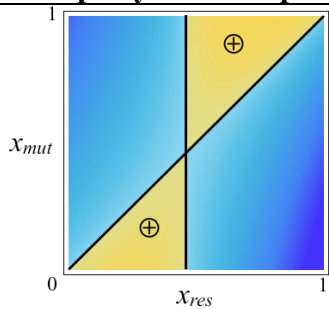
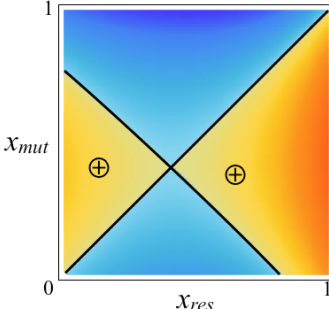
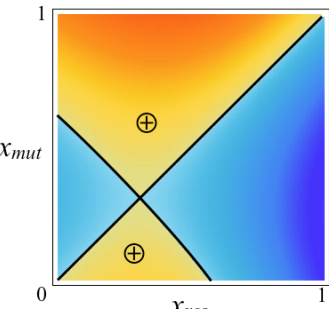
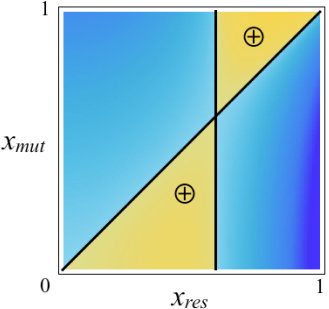
(i) Recovery rate vs. survival

Trade-off functions	Exemplary invasion plot	Nature of the singularity
Linear functions $\begin{cases} \gamma_m = \gamma_0 (1 - x_m) \\ d_m = d_0 (1 - x_m / 2) \end{cases}$		Evolutionarily stable and convergence-stable
Quadratic recovery rate $\begin{cases} \gamma_m = \gamma_0 (1 - x_m^2) \\ d_m = d_0 (1 - x_m / 2) \end{cases}$		Evolutionarily stable and convergence-stable
Quadratic death rate $\begin{cases} \gamma_m = \gamma_0 (1 - x_m) \\ d_m = d_0 (1 - x_m^2 / 2) \end{cases}$	 <p>$\alpha_f = \alpha_m = 0.3$</p>	Evolutionarily unstable and convergence-unstable.
	 <p>$\alpha_f = \alpha_m = 0.37$</p>	<p>For a narrow range of parameter values, there are two singular points, both evolutionarily unstable:</p> <ul style="list-style-type: none"> - x_1 is convergence-unstable, - x_2 is convergence-stable. <p>Other parameter values (e.g. higher virulence) result in the two singular points to vanish.</p>
Quadratic functions $\begin{cases} \gamma_m = \gamma_0 (1 - x_m^2) \\ d_m = d_0 (1 - x_m^2 / 2) \end{cases}$		Evolutionarily stable and convergence-stable.

(ii) Relative fecundity during infection vs. survival

Trade-off functions	Exemplary invasion plot	Nature of the singularity
<p>Linear functions</p> $\begin{cases} \varphi_m = 1 - x_m \\ d_m = d_0 (1 - x_m / 2) \end{cases}$	 <p>$\alpha_f = \alpha_m = 0.52$</p>	<p>Evolutionarily stable and convergence-stable; only found over a narrow range of parameter values.</p>
<p>Quadratic fecundity</p> $\begin{cases} \varphi_m = 1 - x_m^2 \\ d_m = d_0 (1 - x_m / 2) \end{cases}$	 <p>$\alpha_f = \alpha_m = 0.4$</p>	<p>Evolutionarily stable and convergence-stable.</p>
<p>Quadratic death rate</p> $\begin{cases} \varphi_m = 1 - x_m \\ d_m = d_0 (1 - x_m^2 / 2) \end{cases}$		<p>Evolutionarily unstable and convergence-unstable.</p>
<p>Quadratic functions</p> $\begin{cases} \varphi_m = 1 - x_m^2 \\ d_m = d_0 (1 - x_m^2 / 2) \end{cases}$	 <p>$\alpha_f = \alpha_m = 0.53$</p>	<p>Evolutionarily stable and convergence-stable; only found over a narrow range of parameter values.</p>

(iii) Recovery vs. relative fecundity during infection

Trade-off functions	Exemplary invasion plot	Nature of the singularity
<p>Linear functions</p> $\begin{cases} \phi_m = x_m \\ \gamma_m = \gamma_0(1 - x_m) \end{cases}$	 <p>$\alpha_f = \alpha_m = 0.25$</p>	Evolutionarily neutral and convergence unstable.
<p>Quadratic recovery</p> $\begin{cases} \phi_m = x_m \\ \gamma_m = \gamma_0(1 - x_m^2) \end{cases}$	 <p>$\alpha_f = \alpha_m = 0.3$</p>	Evolutionarily stable and convergence-stable.
<p>Quadratic fecundity</p> $\begin{cases} \phi_m = x_m^2 \\ \gamma_m = \gamma_0(1 - x_m) \end{cases}$	 <p>$\alpha_f = \alpha_m = 0.3$</p>	Evolutionarily unstable and convergence-unstable.
<p>Quadratic functions</p> $\begin{cases} \phi_m = x_m^2 \\ \gamma_m = \gamma_0(1 - x_m^2) \end{cases}$	 <p>$\alpha_f = \alpha_m = 0.56$</p>	Evolutionarily neutral and convergence unstable.

Appendix S3. Coevolution of the ‘female’ and ‘male’ traits.

In order to simulate coevolution at the two loci, we adapted the approach the method used by Restif & Koella (2004). As explained by Best et al. (2009), evolutionary stability naturally extends to coevolutionary models, whereas convergence stability can be more complicated to demonstrate. We resort to the following numerical algorithm to determine coevolutionarily stable strategies for the two traits x_f and x_m . First we estimate the ESS of trait x_f for a given value of trait x_m ; then the corresponding ESS of trait x_m ; then use the latter to update the ESS of trait x_f , and carry on iteratively until the two values converge.

An advantage of this method is that each step is just an implementation of the previous ESS algorithm. Because the two traits are not changed simultaneously, we do not need to consider recombination between the two loci.

Fig. S2.1 below illustrates how the coevolutionary stable strategy can be deduced graphically from the two sex-specific ESS.

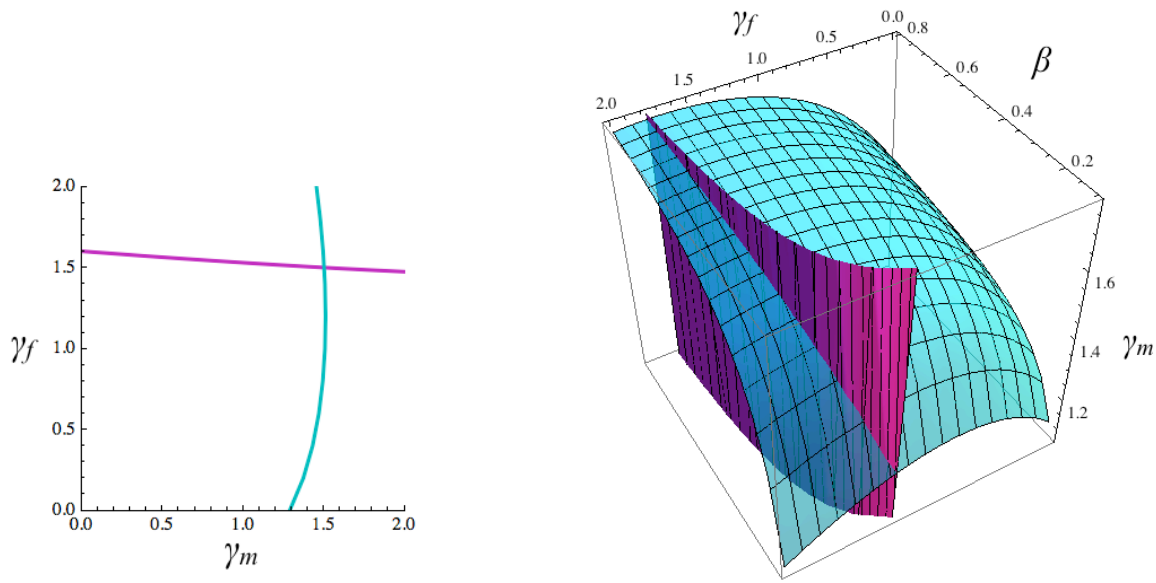


Figure S2.1. Illustration of the coevolutionary stable strategy (CoESS) using model (i) (trade-off between recovery rate γ and natural mortality d , following equation 3i in the main text). Left panel: the purple line was obtained by computing the female ESS x_f^* against a range of male genotypes x_m , and the cyan line was obtained by computing the male ESS x_m^* against a range of female genotypes x_f , then the two curves were plotted as γ_f against γ_m , using the following relations:

$$\begin{cases} \gamma_f = \gamma_0(1 - x_f) \\ d_f = d_0(1 - x_f / 2) \end{cases} \quad \begin{cases} \gamma_m = \gamma_0(1 - x_m) \\ d_m = d_0(1 - x_m / 2) \end{cases} . \text{ The CoESS lies at the intersect of the two curves.}$$

Right panel: same principle but the transmission rate $\beta = \beta_f = \beta_m$ was varied along one of the axes. For any pair of values (β, x_m) , the purple surface shows the value of the female ESS γ_f^* . For any pair of values (β, x_f) , the cyan surface shows the value of the male ESS γ_m^* . The intersect of the two surfaces shows the CoESS as (γ_f^*, γ_m^*) against β , corresponding to the solid line on Fig. 2a (left panel).

Appendix S4. ESS variations using a quadratic trade-off for model (i)

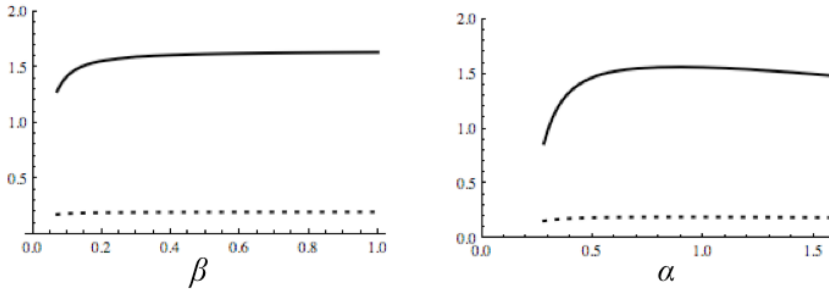
Here we consider a trade-off between recovery and survival (model i) governed by the following functions:

$$\begin{cases} \gamma_f = \gamma_0 (1 - x_f^2) \\ d_f = d_0 (1 - x_f / 2) \end{cases} \quad \begin{cases} \gamma_m = \gamma_0 (1 - x_m^2) \\ d_m = d_0 (1 - x_m / 2) \end{cases} \quad (\text{S4 i})$$

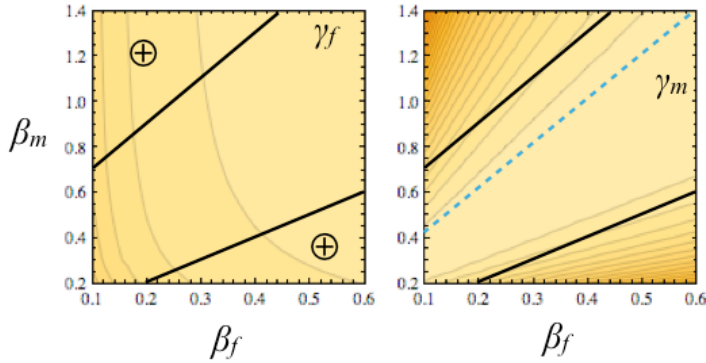
As shown in Appendix S2, these functions enable the existence of ESS. We calculated and plotted the variations of the male and female ESS caused by variations in sex-specific susceptibility or virulence using equations (S4 i), just as we did in the main text using equation (3 i).

1. No sex-specific differences (same legend as Fig. 2)

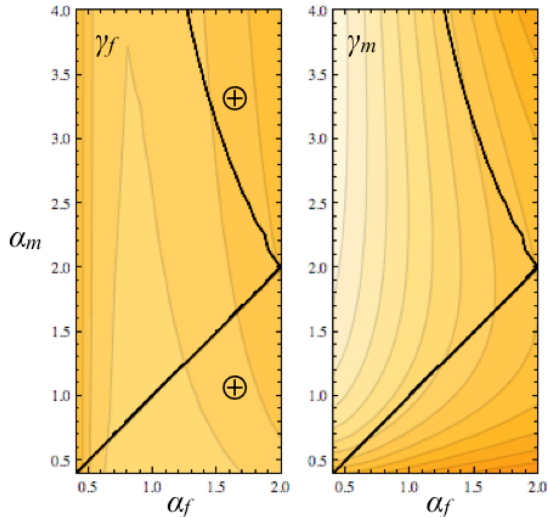
Model (i): γ (—) and d (···)



2. Effect of sex-specific susceptibility (same legend as Fig. 3)



3. Effect of sex-specific virulence (same legend as Fig. 5)



Appendix S5. ESS variations using a linear trade-off for model (ii)

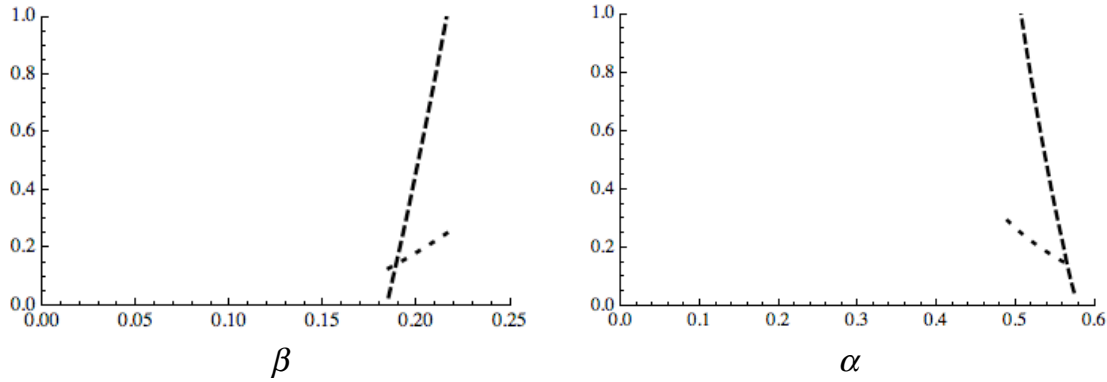
Here we consider a trade-off between relative fecundity during infection and survival (model ii) governed by the following linear functions:

$$\begin{cases} \varphi_f = 1 - x_f \\ d_f = d_0 (1 - x_f / 2) \end{cases} \quad \begin{cases} \varphi_m = 1 - x_m \\ d_m = d_0 (1 - x_m / 2) \end{cases} \quad (\text{S5 ii})$$

As shown in Appendix S2, these functions enable the existence of ESS, albeit only over a narrow range of parameter values. We calculated and plotted the variations of the male and female ESS caused by variations in sex-specific susceptibility or virulence using equations (S5 ii), just as we did in the main text using equation (3 ii).

1. No sex-specific differences (same legend as Fig. 2)

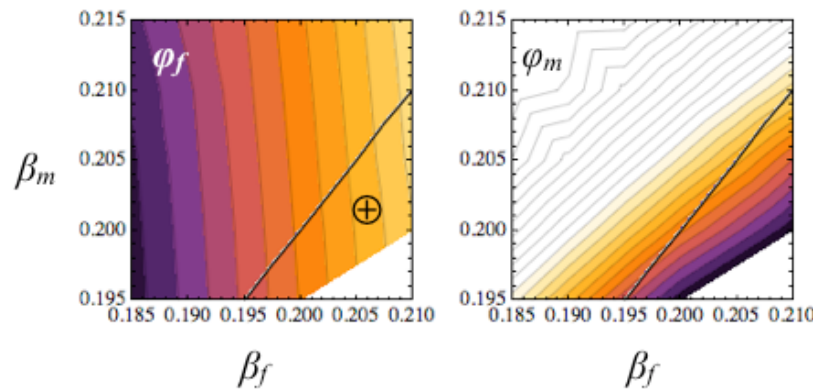
Model (ii): φ (—) and d (· · ·)



Numerical values as in table 1, except $\alpha_f = \alpha_m = 0.54$ (left panel), $\beta_f = \beta_m = 0.178$ (right panel).

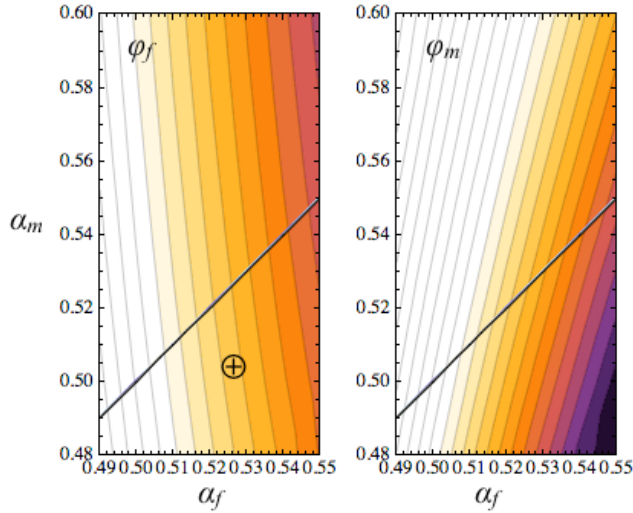
Over the range of values that raise ESS, we observe the same qualitative effects of transmission rate β (increase in ES tolerance) and virulence α (decrease in ES tolerance) as with model (3ii). If we allow negative values of x_f and x_m , then high values of transmission rate or low values of virulence select for ES levels of relative fecundity φ greater than one, meaning that infected individuals have a higher fecundity than uninfected individuals. This phenomenon, known as over-compensation and sometimes observed in plants in response to herbivory (Agrawal 2000) or infection (Salvaudon et al. 2008), has not, to our knowledge, been reported in animals.

2. Effect of sex-specific susceptibility (same legend as Fig. 3)

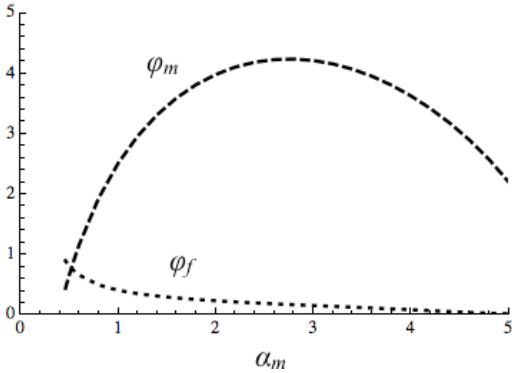


Over the narrow range of parameter values that raise CoESS, we observe that the sex with higher susceptibility evolves higher tolerance, just as on Figure 3.

3. Effect of sex-specific virulence (same legend as Fig. 5)



Over the narrow range of parameter values that raise CoESS, we observe that the sex that suffers higher virulence evolves higher tolerance, as on Figure 5. Besides, the investment in tolerance generally decreases as virulence increases (following the ecological feedback as explained in the main text), with the exception of males investing more when their own virulence increases, at least for low values of virulence, which was also the case with the non-linear model (Fig. 5). The figure below shows that the ES investment in male tolerance (dashed line) actually decreases when virulence becomes high enough (and provided that we allow for ‘over-compensation’, i.e. values of $\phi_m > 1$), in agreement with Fig. 5.



Appendix S6. ESS variations with sex-specific cost of immunity

Here we explore the effects of quantitative variations in the cost of immunity on the ESS of the two sexes.

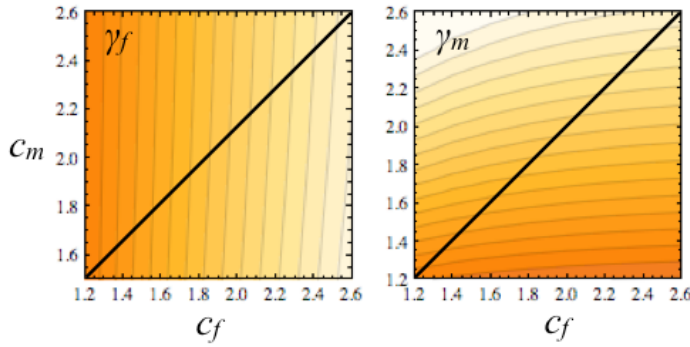
1. Model (i): recovery vs. survival

The trade-off functions are now given by

$$\begin{cases} \gamma_f = \gamma_0 (1 - x_f) \\ d_f = d_0 (1 - x_f / c_f) \end{cases} \quad \begin{cases} \gamma_m = \gamma_0 (1 - x_m) \\ d_m = d_0 (1 - x_m / c_m) \end{cases}$$

where c_f and c_m are arbitrary parameters representing the relative cost of immunity for females and males. For example, all else being equal, if $c_m > c_f$, males suffer a higher mortality than females for the same investment in immunity.

The figure below shows the ESS of females (left) and males (right) against a range of values of c_f (horizontal axis) and c_m (vertical axis); lighter shades represent higher values of the evolutionarily stable recovery rate. As can be understood intuitively, the sex with the higher cost evolves lower recovery rate.

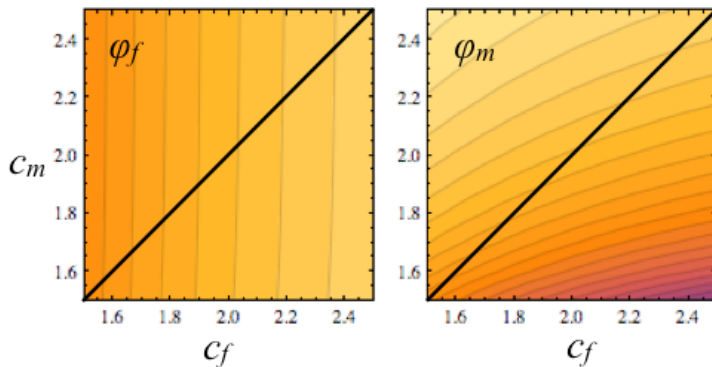


2. Model (ii): relative fecundity during infection vs. survival

The trade-off functions are now given by

$$\begin{cases} \phi_f = 1 - x_f^2 \\ d_f = d_0 (1 - x_f / c_f) \end{cases} \quad \begin{cases} \phi_m = 1 - x_m^2 \\ d_m = d_0 (1 - x_m / c_m) \end{cases}$$

with sex-specific cost of immunity, just as in the previous section. The figure below shows the ESS of females (left) and males (right), with the same pattern as in the previous section.

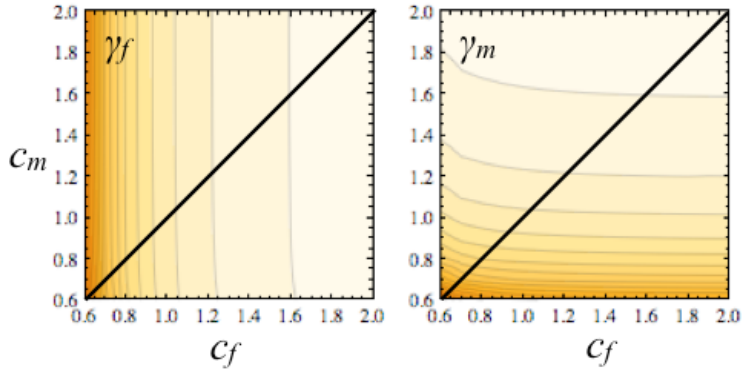


2. Model (iii): recovery vs. relative fecundity during infection

The trade-off functions are now given by

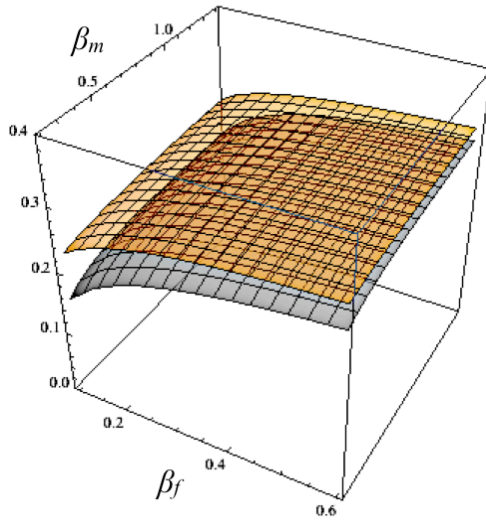
$$\begin{cases} \phi_f = x_f / c_f \\ \gamma_f = \gamma_0 (1 - x_f^2) \end{cases} \quad \begin{cases} \phi_m = x_m / c_m \\ \gamma_m = \gamma_0 (1 - x_m^2) \end{cases}$$

with sex-specific cost of immunity, just as in the previous section. The figure below shows the ESS of females (left) and males (right), with the same pattern as in the previous section.

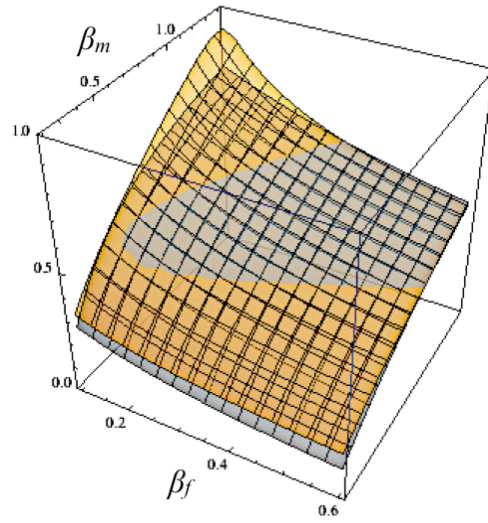


Appendix S7. Effect of sex-specific susceptibility on prevalence.

(a) Female prevalence



(b) Male prevalence



Variations in prevalence (vertical scale) in females (a) and males (b) at equilibrium against female susceptibility β_f and male susceptibility β_m . The grey surfaces were obtained using default numerical values for all other parameters (as in Table 1), whereas the amber surfaces were obtained at the ESS using model (i), as in Fig. 3a.

References for all appendices

- Agrawal, A. A. 2000 Overcompensation of plants in response to herbivory and the by-product benefits of mutualism. *Trends in Plant Science* **5**, 309-313.
- Best, A., White, A. & Boots, M. 2009 The implications of coevolutionary dynamics to host-parasite interactions. *American Naturalist* **173**, 779-791.
- Boots, M. & Haraguchi, Y. 1999 The evolution of costly resistance in host-parasite systems. *The American Naturalist* **153**, 359-370.
- Geritz, S. A. H., Kisdi, E., Mesze, G. & Metz, J. A. J. 1997 Evolutionarily singular strategies and the adaptive growth and branching of the evolutionary tree. *Evolutionary Ecology* **12**, 35-57.
- Restif, O. & Koella, J. C. 2004 Concurrent evolution of resistance and tolerance to pathogens. *The American Naturalist* **164**, E90-E102.
- Salvaudon, L., Héraudet, V. & Shykoff, J. A. 2008 *Arabidopsis thaliana* and the Robin Hood parasite: a chivalrous oomycete that steals fitness from fecund hosts and benefits the poorest one? *Biology Letters* **4**, 526-529.